
Supporting Information

Tunable multicolor fluorescence of polyurethane derivatives induced by molecular weight

Ke-Xin Li,^a Ya-Jie Meng,^b Chang-Yi Zhu,^a Nan Jiang,^{*a} Jia-Wei Xu^{*b} and Yan-Hong Xu^{*a}

^a Key Laboratory of Preparation and Applications of Environmental Friendly Materials, Key Laboratory of Functional Materials Physics and Chemistry of the Ministry of Education (Jilin Normal University), Changchun, 130103, China.

^b Ministry-of-Education Key Laboratory of Numerical Simulation of Large-Scale Complex System (NSLSCS) and School of Chemistry and Materials Science, Nanjing Normal University, Nanjing 210023, China.

E-mails: jiangn270@jlnu.edu.cn; jwxu_njnu@sina.com; xuyh198@163.com

Table of Contents

Experimental details	2
Structural characterization	4
Photophysical properties	5
Theoretical calculations	7
References.....	8

Experimental details

Materials

Materials obtained from commercial suppliers were used without further purification unless otherwise stated. All glassware, syringes, magnetic stirring bars, and needles were thoroughly dried in a convection oven.

Characterization

The UV-vis absorption spectra were recorded on a Shimadzu UV-3100 spectrophotometer. The luminescence movie and photos were taken by an iPhone 14 pro under the irradiation of a hand-held UV lamp at room temperature. ^1H NMR spectra were recorded on a Varian 400 MHz spectrometer. The ^1H NMR spectra were referenced internally to the residual proton resonance in DMSO- d_6 (δ 2.5 ppm). The molecular weights of the polyurethane were determined by gel permeation chromatography (GPC) on a Waters 410 instrument with monodispersed polystyrene as the reference and THF as the eluent at 35°C. Scanning electron microscope (SEM) images were obtained using a JEOL model JSM-6700 instrument operating at an accelerating voltage of 5.0 kV. The samples were prepared by placing microdrops of the solution on a holey carbon copper grid. Steady-state photoluminescence/phosphorescence spectra and phosphorescence lifetime were measured using a Hitachi F-4700 instrument. The fluorescence lifetime was obtained on an Edinburgh FLS-1000 instrument. The photoluminescence quantum efficiency was obtained on a Hitachi F-4700 instrument equipped with the integration sphere. PXRD data were obtained using an Empyrean instrument.

Synthesis of PUB

A mixture of Phenylboronic acid (0.638 g, 5.24 mmol), poly(ethylene glycol) methyl ether ($M_w = 350 \text{ g mol}^{-1}$; 0.792 g, 3.96 mmol), anhydrous THF (4 mL), trimethylhexamethylene diisocyanate (1.652 g, 7.86 mmol) and 1,4-diazabicyclooctane triethylenediamine (DABCO) (0.023 g, 0.21 mmol) was stirred in N_2 atmosphere at 68°C for 8 h until the clear solution became viscous, indicating that polymerization had occurred. After cooling to room temperature, the crude product was added to excess *tert*-butyl methyl ether drop by drop for reverse precipitation to give the end product which was then dried under vacuum at room temperature for 24 h to obtain polyurethane **PUB** (2.2065 g, 60% yield). ^1H NMR (400 MHz, DMSO- d_6 , δ [ppm]): 8.3 (s, 2H), 8.2-7.7 (broad, Benzocyclic hydrogen), 7.5-7.0 (broad, Benzocyclic hydrogen), 7.3 (s, 2H), 4.03 (s, 4H), 3.4-3.6 (broad, PEG protons), 3.23 (s, 6H; PEG terminal -OCH₃ protons), 2.6-3.2 (broad, 4H), 0.5-1.7 (broad, 25H). FT-IR: 3485 cm^{-1} (N-H), 2731 cm^{-1} and 2850 cm^{-1} (-CH₂- asymmetric and symmetric stretch), 1709 (C=O), 1380 (B-O), 1101 cm^{-1} (C-O-C stretch PEG). $M_n=39.48 \text{ kDa}$, $M_w=54.86 \text{ kDa}$, $M_p=43.26 \text{ kDa}$, PDI=1.38.

Synthesis of PUG

A mixture of Phenylboronic acid (0.638 g, 5.24 mmol), poly(ethylene glycol) methyl ether ($M_w = 350 \text{ g mol}^{-1}$; 0.792 g, 3.96 mmol), anhydrous THF (2 mL), anhydrous DMSO (2 mL), trimethylhexamethylene diisocyanate (1.652 g, 7.86 mmol) and 1,4-diazabicyclooctane triethylenediamine (DABCO) (0.023 g, 0.21 mmol) was stirred in N_2 atmosphere at 90°C for 24 h until the clear solution became viscous, indicating that polymerization had occurred. After

cooling to room temperature, the crude product was added to excess *tert*-butyl methyl ether drop by drop for reverse precipitation to give the end product which was then dried under vacuum at room temperature for 24 h to obtain polyurethane **PUG** (2.133 g, 58% yield). ^1H NMR (400 MHz, $\text{DMSO-}d_6$, δ [ppm]): 7.6 (s, 2H), 7.5-7.1 (broad, Benzocyclic hydrogen), 6.5 (s, 2H), 6.4-6.3 (broad, Benzocyclic hydrogen), 4.03 (s, 4H), 3.4-3.6 (broad, PEG protons), 3.23 (s, 6H; PEG terminal $-\text{OCH}_3$ protons), 2.6-3.2 (broad, 4H), 0.5-1.7 (broad, 25H). FT-IR: 3402 cm^{-1} (N-H), 2862 cm^{-1} and 2915 cm^{-1} ($-\text{CH}_2-$ asymmetric and symmetric stretch), 1643 cm^{-1} (C=O), 1378 cm^{-1} (B-O), 1098 cm^{-1} (C-O-C stretch PEG). $M_n=37.07\text{ kDa}$, $M_w=48.90\text{ kDa}$, $M_p=41.12\text{ kDa}$, PDI=1.31.

Synthesis of PUR

A mixture of Phenylboronic acid (0.638 g, 5.24 mmol), poly(ethylene glycol) methyl ether ($M_w = 350\text{ g mol}^{-1}$; 0.792 g, 3.96 mmol), anhydrous DMSO (4 mL), trimethylhexamethylene diisocyanate (1.652 g, 7.86 mmol) and 1,4-diazabicyclooctane triethylenediamine (DABCO) (0.023 g, 0.21 mmol) was stirred in N_2 atmosphere at 150°C for 48 h until the clear solution became viscous, indicating that polymerization had occurred. After cooling to room temperature, the crude product was added to excess *tert*-butyl methyl ether drop by drop for reverse precipitation to give the end product which was then dried under vacuum at room temperature for 24 h to obtain polyurethane **PUR** (2.2433 g, 61% yield). ^1H NMR (400 MHz, $\text{DMSO-}d_6$, δ [ppm]): 6.6 (s, 2H), 6.3 (s, 2H), 6.2-5.6 (broad, Benzocyclic hydrogen), 4.03 (s, 4H), 3.4-3.6 (broad, PEG protons), 3.23 (s, 6H; PEG terminal $-\text{OCH}_3$ protons), 2.6-3.2 (broad, 4H), 0.5-1.7 (broad, 25H). FT-IR: 3385 cm^{-1} (N-H), 2875 cm^{-1} and 2920 cm^{-1} ($-\text{CH}_2-$ asymmetric and symmetric stretch), 1665 cm^{-1} (C=O), 1300 cm^{-1} (B-O), 1095 cm^{-1} (C-O-C stretch PEG). $M_n=19.93\text{ kDa}$, $M_w=25.65\text{ kDa}$, $M_p=14.48\text{ kDa}$, PDI=1.28.

Theoretical calculation

The initial models of three systems (**PUB**, **PUG** and **PUR**) were built by Packmol program and 50 model molecules of PUs ($m = 2$ and $n = 2$) were placed in the box of $60 \times 60 \times 60\text{ \AA}^3$. The model molecular PUs was optimized at the PBE0-D3(BJ)/def2-SVP level of theory¹⁻⁴ using Gaussian 16 (Revision C.01)⁵ and no imaginary frequency was checked by frequency calculation. The restrained electrostatic potential (RESP) atomic charges were generated by Multiwfn.⁶ Force field parameters were adopted from generalized Amber force field (GAFF).⁷ Parameters related to boron were fitted by mSeminario method by Sobtop program.⁸

Molecular dynamics (MD) simulations were performed using the GROMACS (version 2022) package⁹ and topology file and forcefield parameters were created by Sobtop. The long-range electrostatic interactions were handled by the particle-mesh Ewald (PME) method and the cutoff value of van der Waals interactions was set to 10.0 \AA .¹⁰ After energy minimization, the three systems were heated up from 0 K to 300 K in the 2.0 ns simulations. Subsequently, the 50.0 ns MD simulations (MD1) were conducted in the NPT ensemble at 300 K using the v-rescale thermostat method¹¹ and the Parrinello-Rahman barostat.¹² Next, the **PUB**, **PUG** and **PUR** systems were heated up to synthetic temperature 341 K, 363 K and 423 K, respectively, with the 50.0 ns of MD simulations (MD2). Finally, the temperature of the three systems dropped to 300 K and unrestrained MD simulations for 50.0 ns (MD3) were performed.

Natural transition orbitals (NTO) were calculated under NEVPT2(12,12)/def2-TZVP/MM level of theory. Electron-hole distribution was obtained based on NTO results. The

snapshot was taken from MD3 of **PUG** system and optimized under CAM-B3LYP-D3/def2-SVP level of theory by Tci-Chemshell program (version 3.7.1),¹³ where QM region was treated by ORCA program (version 5.0.4)¹⁴ and MM region was treated by DL_poly program¹⁵ with electrostatic embedding scheme. Active spaces used for multi-reference calculation was selected by standard workflow of MOKIT¹⁶ based on the optimized structure, including: 1). RHF/def2-TZVP single point calculation was performed with background charges and wavefunction was checked to be stable by Gaussian16; 2). CIS/def2-TZVP calculation with background charges was performed for lowest 7 states based on previous RHF wavefunction and all excitation components with contribution larger than 10^{-5} were considered and 3). Active spaces were determined based on NTO obtained in CIS calculation.^{17, 18} NEVPT2/MM calculation was performed by PySCF package (version 2.1.1).¹⁹

Structural characterization

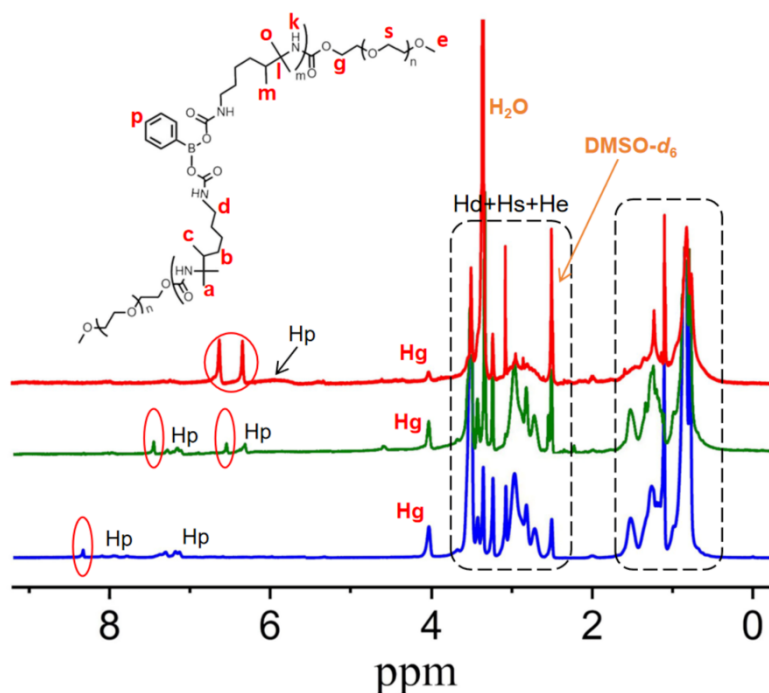


Figure S1. ^1H NMR spectra in $\text{DMSO-}d_6$: from bottom to top **PUB**, **PUG**, **PUR**.

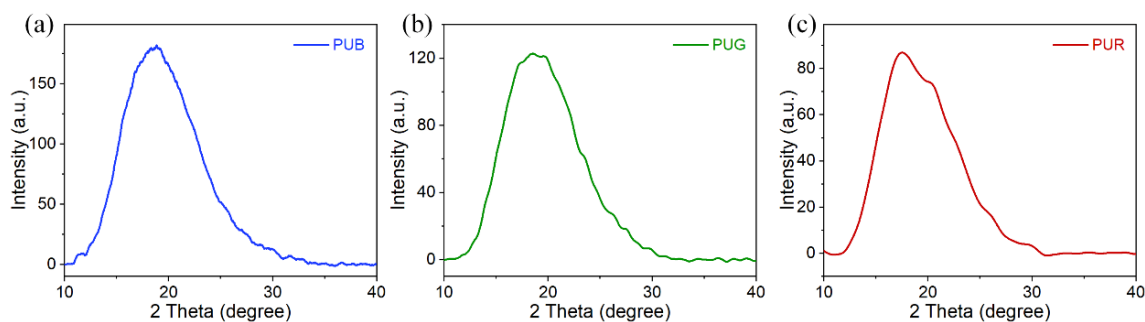


Figure S2. XRD patterns of (a) **PUB**, (b) **PUG** and (c) **PUR**.

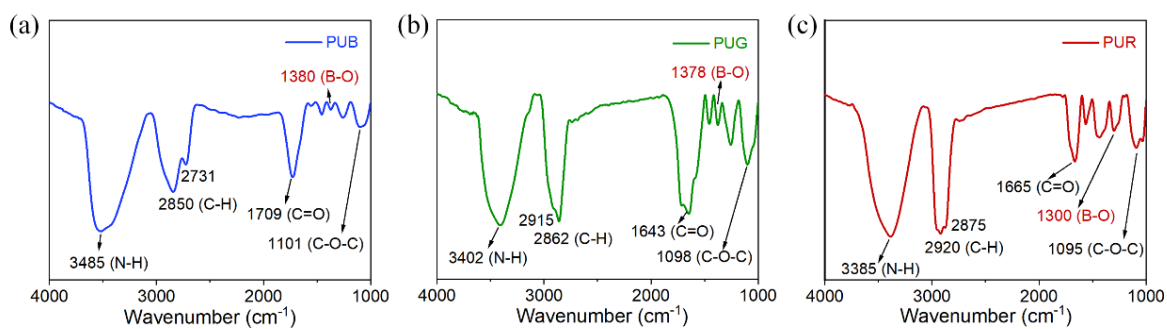


Figure S3. FT-IR spectra of (a) PUB, (b) PUG and (c) PUR.

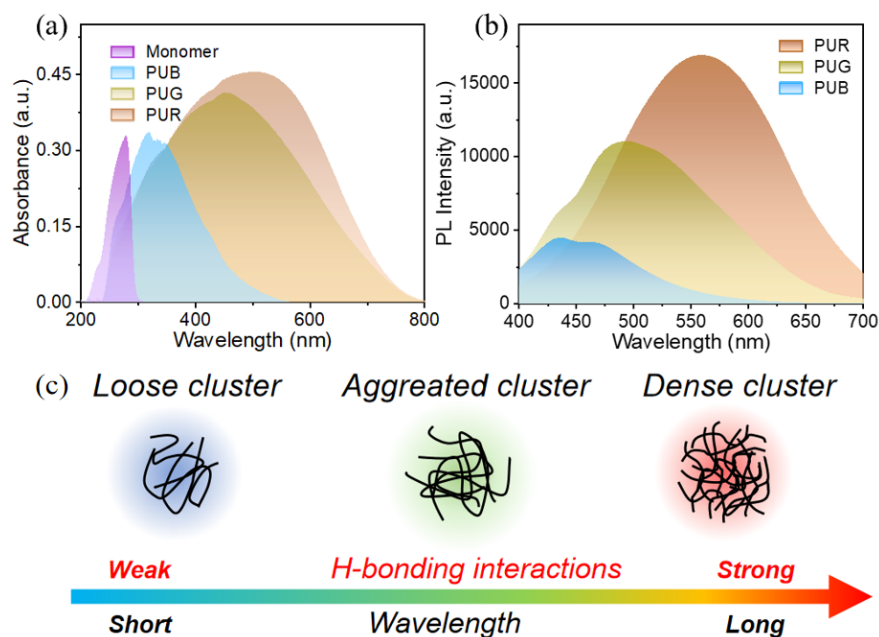


Figure S4. (a) UV-vis spectra of phenylboronic acid monomer, PUs in the solid state. (b) Fluorescence spectra of PUs powders at 365 nm excitation. (c) Schematic diagram of the luminous mechanism of PUs.

Photophysical properties

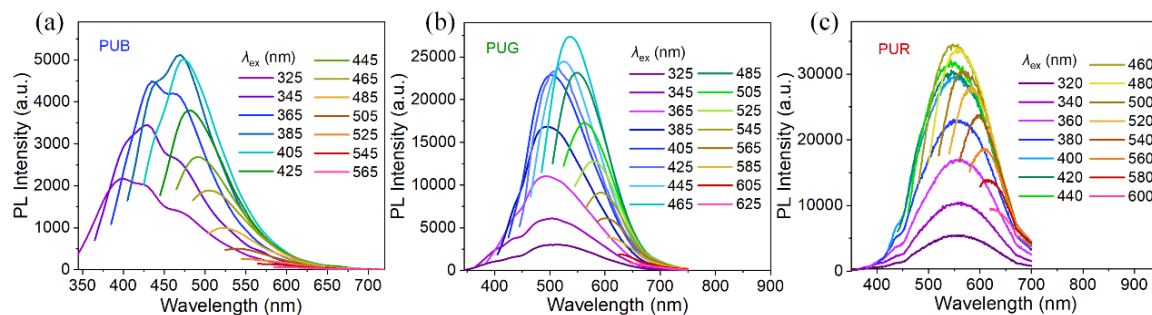


Figure S5. Fluorescence spectra of (a) **PUB**, (b) **PUG** and (c) **PUR** powders at varying λ_{ex} .

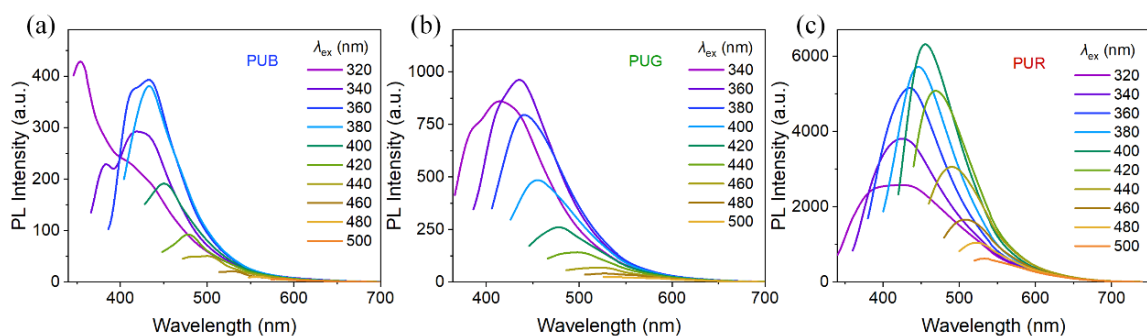


Figure S6. Excitation-dependent emission of (a) **PUB**, (b) **PUG** and (c) **PUR** in DMSO (0.1 mg mL^{-1}) at 365 nm excitation.

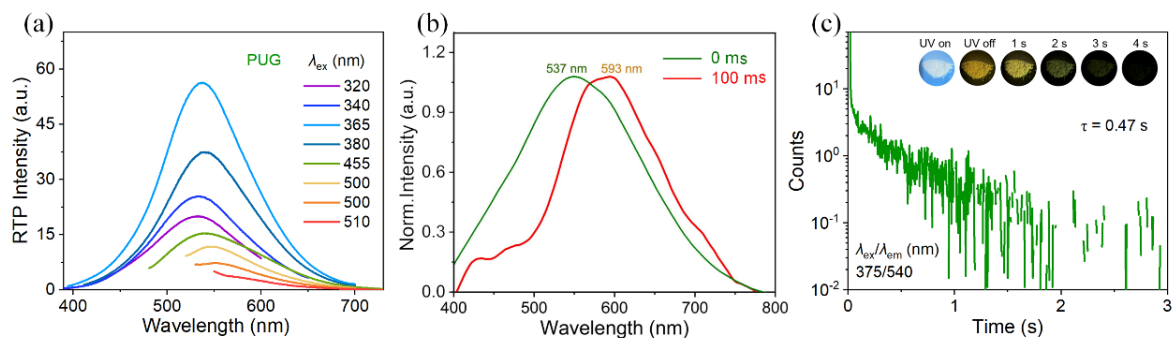


Figure S7. (a) Phosphorescence spectra of **PUG** powder at varying λ_{ex} . (b) Time-resolved delayed spectra of the **PUG** powder sample. (c) Lifetime curve of **PUG**. Insert: phosphorescent images of **PUG** under a 365 nm UV lamp.

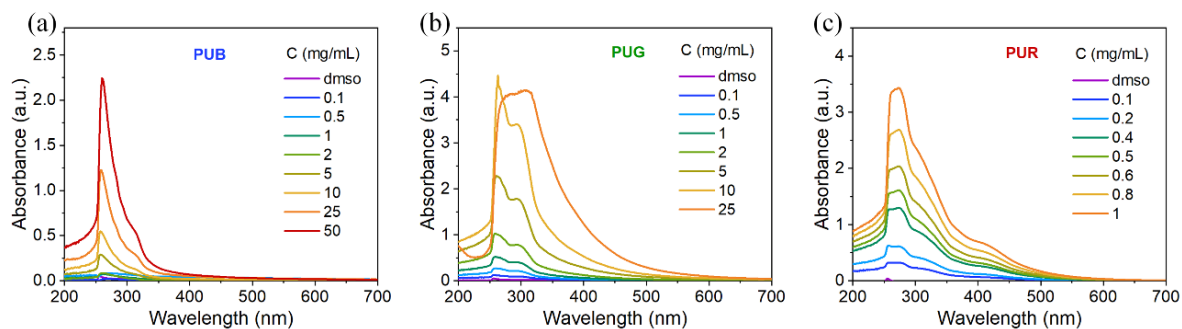


Figure S8. UV-vis absorption spectra of (a) **PUB**, (b) **PUG** and (c) **PUR** in DMSO solution at various concentrations.

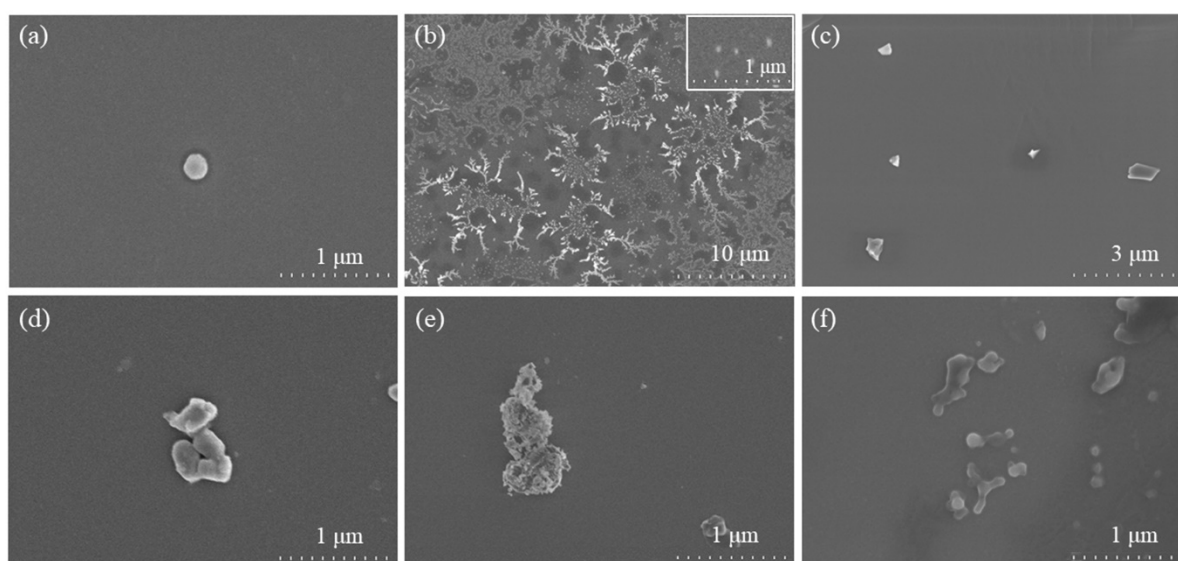


Figure S9. SEM images of (a) **PUB**, (b) **PUG**, (c) **PUR** (0.1 mg mL^{-1}) and (d) **PUB**, (e) **PUG**, (f) **PUR** (2 mg mL^{-1}) in DMSO solution.

Table S1. Summary of physical properties of PUs in the solid state.

	λ_{abs} (nm)	$\lambda_{\text{em}}^{\text{a}}$ (nm)	QY (%)	LT (ns)	M_n^{d} (kDa)	PDI ^d
PUB	327	435	2.6	4.72 ^b /5.17 ^c	39.48	1.38
PUG	438	490	2.1	10.35	37.07	1.31
PUR	509	560	0.2	12.43	19.93	1.27

a: $\lambda_{\text{ex}}=365 \text{ nm}$; b: $\lambda_{\text{ex}}=365 \text{ nm}$, $\lambda_{\text{em}}=435 \text{ nm}$; c: $\lambda_{\text{ex}}=385 \text{ nm}$, $\lambda_{\text{em}}=470 \text{ nm}$; d: number-average molecular weight and polydispersity measured by GPC using THF as the eluent.

Theoretical calculations

Table S2. Stage-average counts of interaction for the whole box (50 molecules) during the three-stage MD simulations.

Interactions	PUB	PUG	PUR
N-H...Acceptor	167/162/170 ^a	157/156/176	164/152/178
C-H...Acceptor	421/428/445	399/394/414	420/382/457

^a For MD1 (initial equilibrium), MD2 (heating) and MD3 (annealing) stage, respectively.

References

1. E. Papajak, H. R. Leverentz, J. Zheng and D. G. Truhlar, *J. Chem. Theory Comput.*, 2009, **5**, 3330-3330.
2. J. P. Perdew, K. Burke and M. Ernzerhof, *Phys. Rev. Lett.*, 1996, **77**, 3865-3868.
3. S. Grimme, *J. Comput. Chem.*, 2006, **27**, 1787-1799.
4. F. Weigend, *Phys. Chem. Chem. Phys.*, 2006, **8**, 1057-1065.
5. M. J. Frisch, G. W. Trucks, H. B. Schlegel, G. E. Scuseria, M. A. Robb, J. R. Cheeseman, G. Scalmani, V. Barone, G. A. Petersson, H. Nakatsuji, X. Li, M. Caricato, A. V. Marenich, J. Bloino, B. G. Janesko, R. Gomperts, B. Mennucci, H. P. Hratchian, J. V. Ortiz, A. F. Izmaylov, J. L. Sonnenberg, Williams, F. Ding, F. Lipparini, F. Egidi, J. Goings, B. Peng, A. Petrone, T. Henderson, D. Ranasinghe, V. G. Zakrzewski, J. Gao, N. Rega, G. Zheng, W. Liang, M. Hada, M. Ehara, K. Toyota, R. Fukuda, J. Hasegawa, M. Ishida, T. Nakajima, Y. Honda, O. Kitao, H. Nakai, T. Vreven, K. Throssell, J. A. Montgomery Jr., J. E. Peralta, F. Ogliaro, M. J. Bearpark, J. J. Heyd, E. N. Brothers, K. N. Kudin, V. N. Staroverov, T. A. Keith, R. Kobayashi, J. Normand, K. Raghavachari, A. P. Rendell, J. C. Burant, S. S. Iyengar, J. Tomasi, M. Cossi, J. M. Millam, M. Klene, C. Adamo, R. Cammi, J. W. Ochterski, R. L. Martin, K. Morokuma, O. Farkas, J. B. Foresman and D. J. Fox, Gaussian 16 Rev. C.01, Wallingford, CT, 2016.
6. T. Lu and F. Chen, *J. Comput. Chem.*, 2012, **33**, 580-592.
7. K. G. Sprenger, V. W. Jaeger and J. Pfaendtner, *J. Phys. Chem. B*, 2015, **119**, 5882-5895.
8. L. Tian, Sobtop, 1.0(dev3.1).
9. B. Hess, C. Kutzner, D. Van Der Spoel and E. Lindahl, *J. Chem. Theory Comput.*, 2008, **4**,

435-447.

10. T. Darden, D. York and L. Pedersen, *J. Chem. Phys.*, 1993, **98**, 10089-10092.
11. G. Bussi, D. Donadio and M. Parrinello, *J. Chem. Phys.*, 2007, **126**.
12. M. Parrinello and A. Rahman, *J. Appl. Phys.*, 1981, **52**, 7182-7190.
13. S. Metz, J. Kästner, A. A. Sokol, T. W. Keal and P. Sherwood, *WIREs Comput. Mol. Sci.*, 2014, **4**, 101-110.
14. F. Neese, *WIREs Comput. Mol. Sci.*, 2022, **12**, e1606.
15. W. Smith, C. W. Yong and P. M. Rodger, *Mol. Simulat.*, 2002, **28**, 385-471.
16. J. Zou, Molecular Orbital Kit (MOKIT). <https://gitlab.com/jxzou/mokit> (accessed 2023. 11. 01).
17. B. S. Fales, Y. Shu, B. G. Levine and E. G. J. Hohenstein, *Chem. Phys.*, 2017, **147**, 094104.
18. Y. Shu, E. G. Hohenstein and B. G. Levine, *J. Chem. Phys.*, 2015, **142**, 024102.
19. Q. Sun, T. C. Berkelbach, N. S. Blunt, G. H. Booth, S. Guo, Z. Li, J. Liu, J. D. McClain, E. R. Sayfutyarova, S. Sharma, S. Wouters and G. K. L. Chan, *WIREs Comput. Mol. Sci.*, 2018, **8**, e1340.